TUPP21

The HL-LHC Beam Gas Vertex Monitor - Simulations for Design Optimisation and Performance Study

B. Kolbinger, H. Guerin[1], O. R. Jones, T. Lefevre J. W. Storey, A. Salzburger, R. Veness, C. Zamantzas, CERN, 1211 Geneva 23, Switzerland
S. M. Gibson, R. Kieffer, Royal Holloway, University of London, Surrey, UK
[1]also at Royal Holloway, University of London, Surrey, UK

Research supported by the High Luminosity LHC project

IBIC 2021 International Beam Instrumentation Conference

1 Introduction

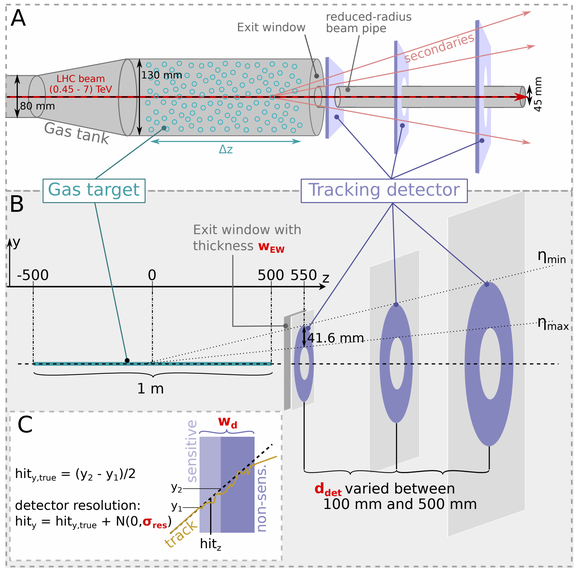

Figure 1: A: BGV sketch. B: Simulation setup. C: Z-y view of a detector layer.

The Beam Gas Vertex (BGV) device is a novel non-invasive beam profile monitor that is currently under development for the High Luminosity upgrade of the Large Hadron Collider (HL-LHC) at CERN. Its challenging goal is to provide a **continuous measurement of the emittance and transverse beam profile throughout the whole LHC cycle (450 GeV to 7 TeV)**.

Beam-gas collision products stemming from LHC protons interacting inelastically with the BGV's gas target installed in the path of each circulating beam, are measured via tracking detectors. The beam profile is determined from the **spatial distribution of the reconstructed vertices of the collisions**.

2 Performance, simulation tools & goals

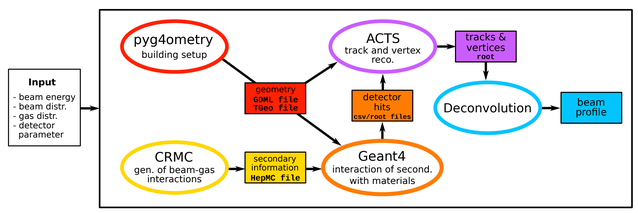

- Based on extensive **simulation studies** and what has been learned from the **BGV demonstrator** [1] & → **design of future BGV**.
- Goal of simulations: **ascertain requirements for tracking detector and gas target within boundary conditions** provided by the feasibility of integrating it into the LHC.
- **Performance measure:** true beam profile is unfolded from spatial distribution of reconstructed vertices and vertex response of the BGV system. Precise knowledge of the vertex response is difficult to achieve → keep its width i.e. the **vertex resolution** σ_v low relative to the true beam width. At the foreseen location of the BGV, the smallest expected beam size will be ≈ 200 µm.
- Estimation of necessary transverse resolution → $\sigma_{x,y} \lesssim 140$ µm [2].
- **Investigate key design parameters (see Fig. 1) via simulations & vertex reconstruction.**

3 Vertex resolution

σ_v depends on characteristics of the measured tracks corresponding to an interaction:

- **Number of tracks**: $\sigma_v \propto \frac{1}{\sqrt{N_{tr}}}$ - which in turn depends on beam energy, gas species, detector coverage and the distance from the interaction vertex to the detector.
- **quality of measured track**, which can be studied via the transverse impact parameter resolution of a single track calculated via [3] $\sigma_{IP}^2 = \sigma_{int,det}^2 + \sigma_{MS}^2$, with the **intrinsic detector contribution** $\sigma_{int,det}$ [4] (dependent on σ_{res} and d_{det}). and the **multiple scattering** σ_{MS} in the materials.

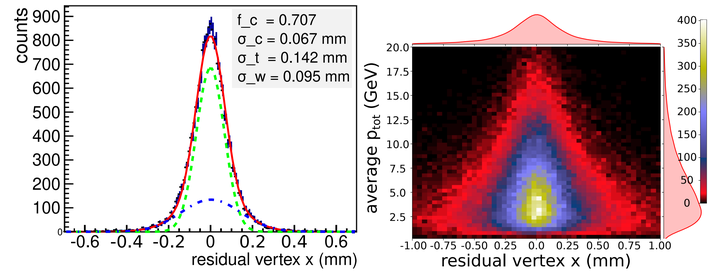

Figure 2: Residual r_x ($N_{tr} = 5$). Red line: fit with sum of two Gaussians. Green and blue dashed lines: core and tail Gaussians. Right: two-dimensional histogram of the r_x ($N_{tr} \geq 2$) vs average total momentum of the tracks stemming from the vertex.

Determining the vertex resolution:

- **Reconstruct tracks and vertices via ACTS** (A Common Tracking Software) [5, 6]. Tracks are fitted via a Kalman Fitter [7]. Afterwards, the fitted tracks are used to determine the vertex with the Billoir fitter [8].
- Compute residuals $r_i = v_{i,fit} - v_{i,true}$ with $i = \{x, y, z\}$. **Fit residuals with a sum of two Gaussians** (core and tail Gaussian [9]) with widths σ_c and σ_t. The vertex resolution can then be calculated as the weighted average $\sigma_v = \sqrt{f_c\sigma_c^2 + f_t\sigma_t^2}$, where f_c and f_t are core and tail fractions, calculated via: $f_t = \frac{p_t\sigma_c}{p_c\sigma_c + p_t\sigma_t}$, where p denotes the amplitudes and σ the widths of the Gaussians.

4 Vertex resolution vs number of tracks (N_{tr})

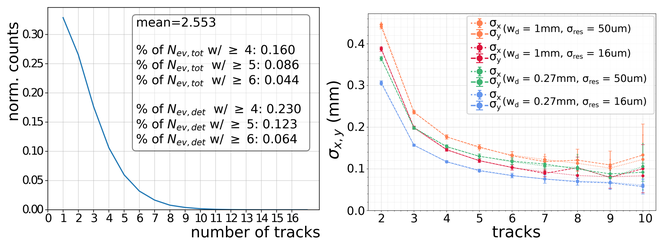

Figure 4: Left: histogram of N_{tr} (450 GeV) for 500 000 events. Right: $\sigma_{x,y}$ versus N_{tr} for different detector cases. The size of the error bars is calculated via error propagation of the fit errors on σ_c, σ_t, p_c and p_t. They increase with higher N_{tr} due to lower event statistics.

- d_{det} has been fixed to 250 mm and results for detector resolutions $\sigma_{res} = \{16, 50\}$ µm and $w_d = \{1, 0.27\}$ mm are shown.

5 Vertex resolution vs distance between detector layers (d_{det})

- For $\sigma_{res} = 50$ µm (orange and purple), a significant increase in resolution is observed with d_{det}.
- for $\sigma_{res} = 16$ mu, the gain in $\sigma_{x,y}$ is less prominent and shows convergence at about 250 mm.
- These results indicate that a detector with a high spatial resolution such as a Si pixel detector could allow for a more compact detector design.

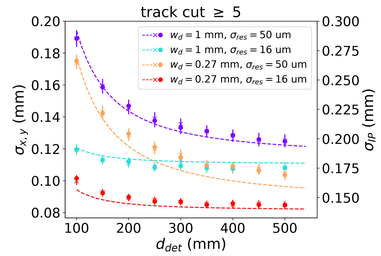

Figure 3: $\sigma_{x,y}$ for events with $N_{tr} \geq 5$ (points) and calculated σ_{IP} (dashed line) as a function of d_{det}.

6 Exit window thickness (w_{EW})

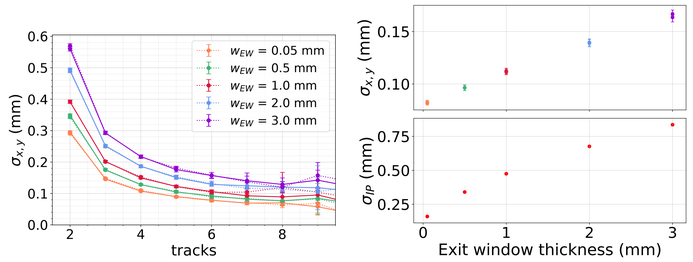

Figure 5: Left: $\sigma_{x,y}$ in dependence of N_{tr} for different window thicknesses. Right: comparison of $\sigma_{x,y}$ (top) and calculated σ_{IP} (bottom) versus w_{EW}.

- Window thicknesses $w_{EW} = \{0.05, 0.5, 1, 2, 3\}$ mm for a detector with $d_{det} = 250$ mm, $w_d = 1$ mm and $\sigma_{res} = 16$ µm.

7 Vertex resolution vs distance between vertex and detector

- A detector with $d_{det} = 250$ mm, $w_d = 0.27$ mm and $\sigma_{res} = 16$ µm is used.
- The vertices are grouped together to bins with a width of 100 mm, as indicated by the x-axis labels. The data points show the average $\sigma_{x,y}$ of events belonging to the same bin and $N_{tr} \geq 5$ (Fig. 6 top).
- The resolution decreases with distance, however, this effect is lessened due to the increase of average track momenta (Fig. 6 centre) for events further away from the detector.

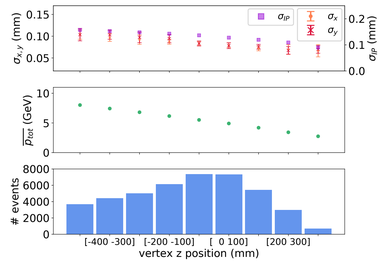

Figure 6: $\sigma_{x,y}$ and σ_{IP} (top), the average track momentum (middle), and the number of events (bottom) as a function of the vertices z-position.

References

[1] A. Alexopoulos et al. "Noninvasive LHC transverse beam size measurement using inelastic beam-gas interactions". In: *Physical Review Accelerators and Beams* 22.4 (Apr. 2019), p. 042801. DOI: 10.1103/PhysRevAccelBeams.22.042801.

[2] H. Guerin et al. "The HL-LHC Beam Gas Vertex Monitor - Simulations for Design Optimisation and Performance Study". In: *presented at IPAC'21* (Campinas, Brazil). JACoW Publishing, May 2021.

[3] Andreas Salzburger. "A parametrization for fast simulation of muon tracks in the ATLAS inner detector and muon system". MA thesis. Innsbruck U., 2003.

[4] F Ragusa and L Rolandi. "Tracking at LHC". In: *New Journal of Physics* 9.9 (Sept. 2007), pp. 336–336. DOI: 10.1088/1367-2630/9/9/336.

[5] Xiaocong Ai et al. "A Common Tracking Software Project", submitted to *Computing and Software for Big Science* on 25 Jun 2021. 2021. URL: https://arxiv.org/abs/2106.13593.

[6] *ACTS on GitHub*. https://github.com/acts-project/acts. Accessed: 2021-08-27.

[7] R. E. Kalman. "A New Approach to Linear Filtering and Prediction Problems". In: *Journal of Basic Engineering* 82.1 (Mar. 1960), pp. 35–45. DOI: 10.1115/1.3662552.

[8] P. Billoir and S. Qian. "Fast vertex fitting with a local parametrization of tracks". In: *Nuclear Inst. and Methods in Physics Research, A* 311.1-2 (1992), pp. 139–150. DOI: 10.1016/0168-9002(92)90859-3.

[9] *Performance of tracking and vertexing techniques for a disappearing track plus soft track signature with the ATLAS detector*. Tech. rep. Geneva: CERN, Mar. 2019.